Article

Not peer-reviewed version

Experimental and Statistical Analysis of the Effect of Heat Treatment on Surface Roughness and Mechanical Properties of Thin-Walled Samples Obtained by Selective Laser Melting from the Material AlSi10Mg

Sergey N. Grigoriev , Nikita Yu. Nikitin * , Oleg Yanushevich , Natella Kriheli , Olga Kramar , Roman Khmyrov , Idarmach Idarmachev , Pavel Peretyagin

Posted Date: 19 October 2023

doi: 10.20944/preprints202310.1275.v1

Keywords: selective laser melting; aluminum alloys; surface roughness; heat treatment; mechanical properties

Article

Experimental and Statistical Analysis of the Effect of Heat Treatment on Surface Roughness and Mechanical Properties of Thin-Walled Samples Obtained by Selective Laser Melting from the Material AlSi10Mg

Sergey N. Grigoriev [1], Nikita Nikitin [1,*], Oleg Yanushevich [2], Natella Kriheli [2], Olga Kramar [2], Roman Khmyrov [3], Idarmach Idarmachev [3] and Pavel Peretyagin [1,2]

[1] Spark Plasma Sintering Research Laboratory, Moscow State University of Technology "STANKIN", Vadkovsky per. 1, Moscow, Russian Federation s.grigoriev@stankin.ru (S.N.G.); nikitin5@yandex.ru (N.N.); p.peretyagin@stankin.ru (P.P.)

[2] Federal State Budgetary Educational Institution of the Higher Education "A.I. Yevdokimov Moscow State University of Medicine and Dentistry" of the Ministry of Healthcare of the Russian Federation, Moscow, Russian Federation; olegyanushevich@mail.ru (O.Y.); nataly0088@mail.ru (N.K.); dr.ovkramar@gmail.com (O.K.)

[3] Laboratory of Innovative Additive Technologies, Moscow State University of Technology "STANKIN", Vadkovsky per. 1, Moscow 127055, Russian Federation r.khmyrov@stankin.ru (R.K.); _idarmachev_@mail.ru (I.I.)

* Correspondence: nikitin5@yandex.ru

Abstract: Statistical analysis of mechanical properties of thin-walled samples (~500 microns) obtained by selective laser melting from AlSi10Mg material and subjected to heat treatment for 1 hour at temperatures from 260 °C to 440 °C (step of aging temperature change 30 °C) has shown that the maximum strain hardening in the stretching diagram section from yield strength to tensile strength is achieved at the heat treatment temperature equal to 290 °C. At carrying out of correlation analysis statistically significant positive correlation between deformation corresponding to yield strength and the sum of heights of the largest protrusions and depths of the largest depressions of the surface roughness profile within the basic length of the sample (Rz) and the full height of the surface roughness profile (Rmax) was established. It was found that the reason for the correlation is the presence of cohesive states between the extreme values of the surface roughness profile that persist along the entire length of the specimen.

Keywords: selective laser melting; aluminum alloys; surface roughness; heat treatment; mechanical properties

1. Introduction

One of the main directions of development of modern industrial technologies is the creation of high-quality products with low production costs. Reduction of production costs can be achieved by reducing to the minimum possible time of creation of the final product - "from idea to finished product" with simultaneous preservation of high quality of manufacturing. Among the technologies actively introduced in the production process, additive manufacturing technologies fall under these requirements.

ISO/ASTM 52900:2015 classifies the technologies used in additive manufacturing and considers the type of raw materials, deposition techniques and methods of melting or curing the material [1]. The most common technologies of additive manufacturing are SLA and FDM printing [2–6], these technologies use thermoplastics and polymer resins as the main materials, which limits the scope of application of products made by these technologies. Technologies that allow manufacturing products from metal, such as selective laser melting (SLM) technology [7–15], have a wider industrial potential.

 doi:10.20944/preprints202310.1275.v1

Powders of metals and alloys of various compositions are used as a starting material to produce final products using selective laser melting technology. In the presented work, samples made by SLM technology from light alloy AlSi10Mg were studied.

AlSi10Mg has good mechanical strength, corrosion resistance [16–19] and allows to manufacture products using SLM technology of complex geometric shape [20]. Kamarudin, K., et al [20] note that during the manufacture of complex-shaped products (molds), inhomogeneity of surface roughness and deviation of actual dimensions from the design dimensions are observed, which is attributed to the influence of local heat transfer. Studies [21,22] show that the effect of local heat transfer affects the microstructure of the bulk product and, consequently, the mechanical properties. In addition, the change in mechanical properties of the final product depends on the tilt angle of the product during printing. Changing the tilt angle from 35.5° to 90° leads to an increase in mechanical properties by 12% (as the angle increases), while the surface roughness decreases [21].

Increase of mechanical properties at manufacturing of specimens by SLM technology from AlSi10Mg material is achieved due to hardening. The main mechanism of hardening is precipitate hardening, which contributes more than hardening of Si solid solution in α-Al matrix [22]. Clarification of the mechanisms of mechanical property enhancement of AlSi10Mg samples obtained by selective laser melting shows that precipitate strengthening is achieved due to a very thin Al-Si eutectic structure between α-Al dendrites and the formation of a microstructure oriented transversely to the direction of load application, and the anisotropy of properties becomes minimal when the scanning speed is optimized [23–25]. Additional sources of improvement of mechanical properties of the samples are changes in the gas atmosphere in which selective laser melting is performed, changes in surface roughness and porosity, as well as thermal post-treatment of parts manufactured by SLM printing technology from AlSi10Mg. When argon was replaced by nitrogen in the working chamber of the SLM 3D printer, the achievement of the strength limit of ~350 MPa was recorded [25].

The influence of porosity and surface roughness of the samples obtained by SLM printing technology from AlSi10Mg has received a great deal of attention [26–44]. The focus of the works is related to the optimization of technological parameters to reduce surface roughness and porosity and, consequently, to increase hardness, impact toughness and fatigue strength by reducing the surface roughness of samples obtained by SLM printing technology from AlSi10Mg. In particular, the critical point of energy density, which gives the minimum pore fraction for AlSi10Mg and is about 60 J/m3 [37] and exposure time of 140-160 μs [38], was shown to exist. In addition to the optimization of technological parameters, the influence of different surface post-treatment methods on the mechanical properties of samples has been investigated [42,43]. It is noted in [42] that strong vibration hardening had the greatest effect on the improvement of fatigue life, followed by laser hardening and shot peening.

However, the works do not analyze the changes in tensile mechanical properties as a function of surface roughness on thin-walled samples, where the contribution of the surface to the tensile strength may be significant.

The influence of thermal post-treatment on the mechanical properties of samples produced by SLM technology is under active study [45] and requires detailed elaboration. In the works [30,46] the application of standard heat treatment T6 is considered, and it is shown that the average surface roughness of samples obtained by SLM technology from AlSi10Mg material decreased after heat treatment at 540 °C for 2 h. However, after artificial aging at 155 °C for 12 h and initially at 530 °C for 2 h, the surface roughness increased [30]. The lack of significant hardening of the material under the standard T6 heat treatment regime is also confirmed [46]. In [47], the occurrence of anisotropy of mechanical properties arising in horizontally annealed samples during heat treatment carried out at 270 °C for 1.5 h was demonstrated, and a decrease in properties compared to non-annealed samples was observed, indicating the need for further search for an optimal heat treatment regime.

Thus, the purpose of the presented work is to determine the effect of heat treatment at temperatures from 260 °C to 440 °C for 1 hour on the tensile mechanical properties and surface roughness of thin-walled samples (~500 μm) manufactured by SLM technology from AlSi10Mg.

Preprints (www.preprints.org) | NOT PEER-REVIEWED | Posted: 19 October 2023 doi:10.20944/preprints202310.1275.v1

2. Materials and Methods

2.1. Physical and mechanical properties

The microstructure and chemical composition of the studied materials were analyzed using a Phenom ProX scanning electron microscope (Holland) equipped with an adapter for elemental analysis by energy dispersive spectroscopy. X-ray diffraction (XRD) analysis was used to determine the phase composition of the samples. X-ray diffractograms were obtained on a PANalytical Empyrean X-ray diffractometer with CuKa radiation. The phase composition was analyzed using PANalytical High Score Plus software, software [48] and ICCD PDF-2 and COD databases [49]. The surface roughness of the samples was measured using a HOMMEL-ETAMIC T8000 profilograph (JENOPTIK (Hommel-Etamic), Jena, Germany). Mechanical tensile tests were performed on an INSTRON 5989 electromechanical testing machine (Instron, Norwood, MA, USA) at a speed of 2mm/min. Statistical analysis of the experimental results was performed using software (Rstudio 2023.06.1 Posit Software, PBC, GNU license) written in R language.

2.2. Production of samples

AlSi10Mg powder served as a starting material for the fabrication of samples by selective laser melting. The size of the powders ranged from 30 μm to 75 μm. Figure 1 shows a micrograph of the starting material and the size distribution of the powder particles.

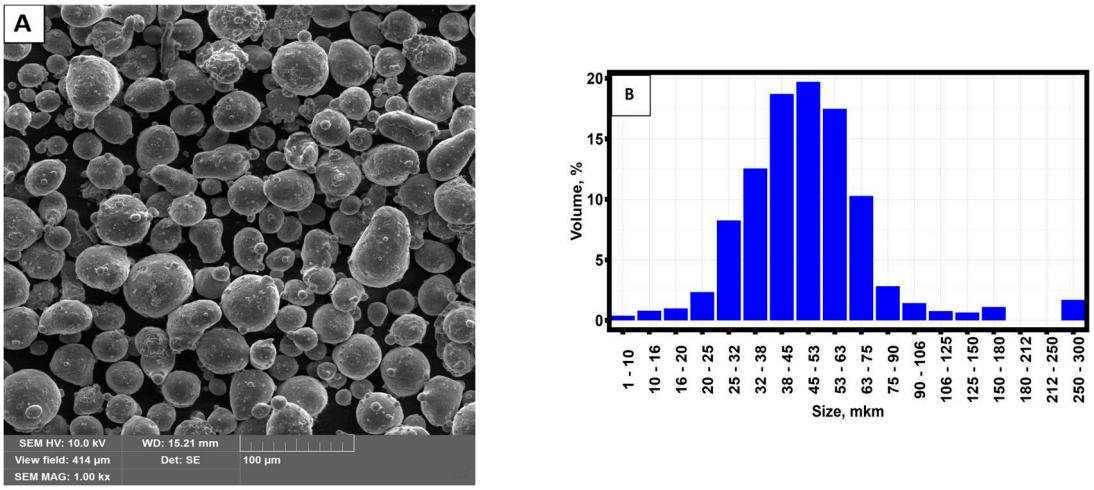

Figure 1. (**A**) SEM image of the initial AlSi10Mg powder. (**B**) Particle size distribution.

The average chemical composition of the initial AlSi10Mg powder is presented in Table 1.

Table 1. Average chemical composition of AlSi10Mg powder.

Elements	Al	Si	Mg	O
Composition (wt %)	88.1850	9.9550	0.3275	1.5325

Printing was carried out on a Farsoon FS121M SLM selective laser melting machine (Farsoon Technologies, Hunan, China) with a pre-installed laser with a maximum power of 500W. The main printing modes were layer thickness 30 μm, laser power P = 340 W, hatching distance - 0.15 mm, laser travel speed - 1500 mm/sec. Figure 2 shows a schematic drawing of the sample and its location on the table during fabrication by selective laser melting.

Preprints (www.preprints.org) | NOT PEER-REVIEWED | Posted: 19 October 2023 doi:10.20944/preprints202310.1275.v1

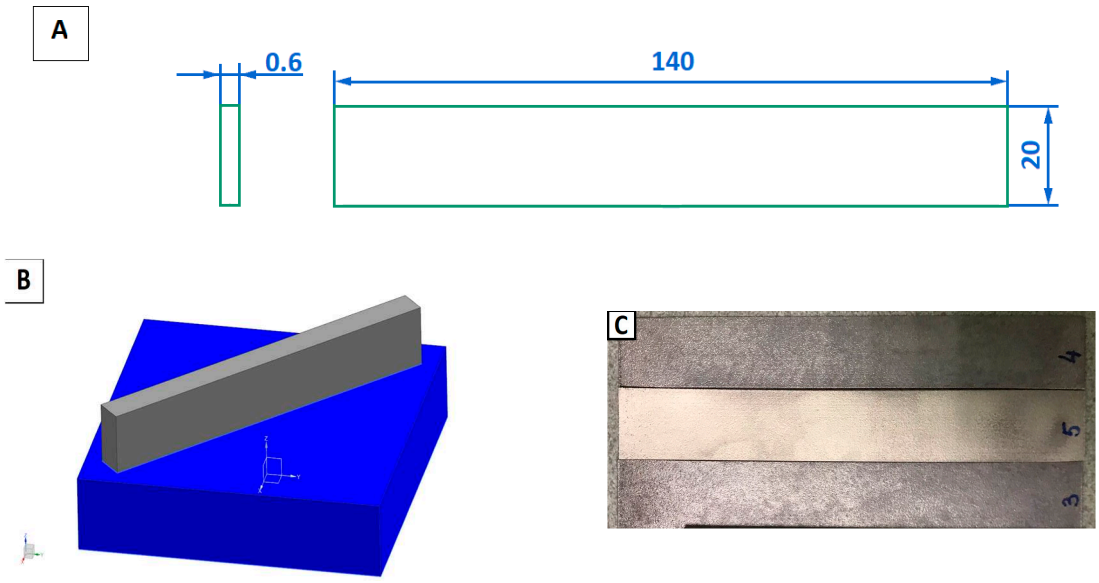

Figure 2. Schematic parameters of the sample made by selective laser melting method (**A**), its location on the table during printing (**B**) and samples made by selective laser melting method (**C**).

3. Results and discussions

3.1. Surface roughness of samples manufactured by selective laser melting technology from AlSi10Mg material.

48 samples made by selective laser melting technology from AlSi10Mg material were subjected to surface roughness study.

Figure 3 shows the results of surface roughness profile measurements for the samples that were not annealed after fabrication by selective laser melting technology. Similar roughness diagrams were obtained for the other 42 samples.

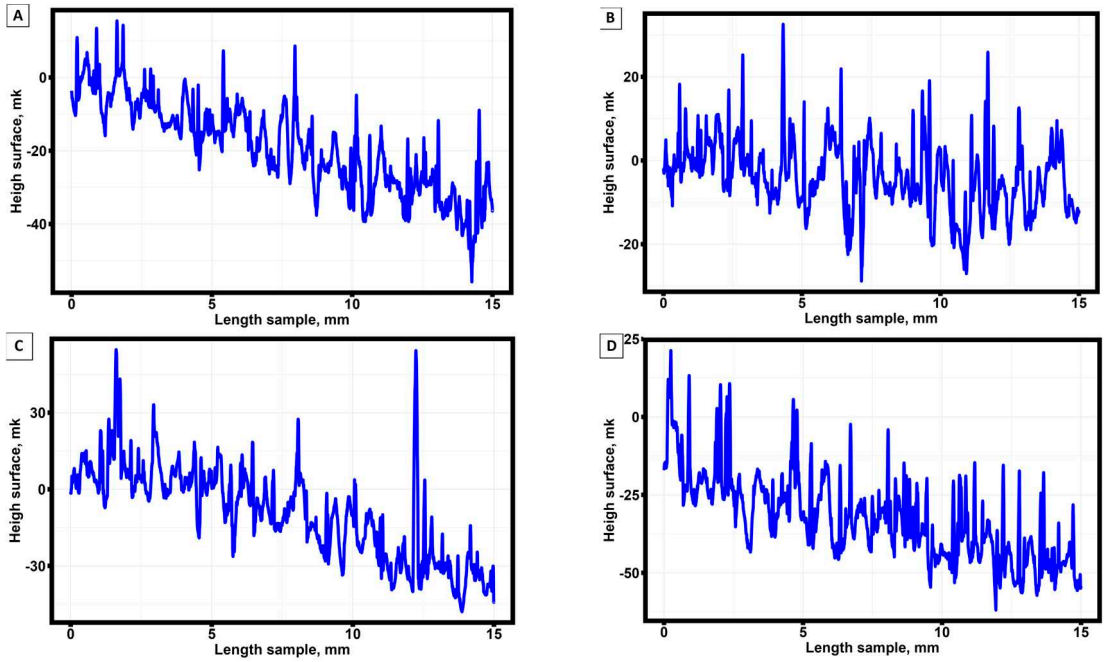

Preprints (www.preprints.org) | NOT PEER-REVIEWED | Posted: 19 October 2023 doi:10.20944/preprints202310.1275.v1

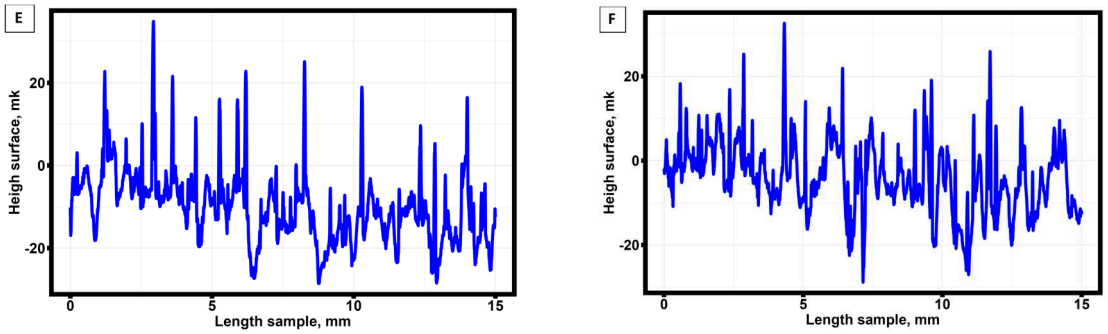

Figure 3. Surface profile for six unannealed samples. (**A**) sample No 1; (**B**) sample No 2; (**C**) sample No 3; (**D**) sample No 4; (**E**) sample No 5; (**F**) sample No 6.

The analysis of the autocorrelation functions of the surface profile shows that there is a regularity in the variation of the surface profile height depending on the sample length, which has the character of a stationary series [50].

Table 2 presents the arithmetic mean values of the absolute values of profile deviations within the base length (Ra), the sum of the height of the largest profile protrusion and the depth of the largest profile depression within the base length of the sample (Rz) and the total profile height (Rmax) of all samples.

Table 2. Surface roughness of samples produced by selective laser melting technology from AlSi10Mg.

No samples	Annealing temperature, °C	Ra, μm	Rz, μm	Rmax, μm
1	20	4,208	33,040	41,141
2	20	5,996	49,628	63,651
3	20	7,340	54,939	93,837
4	20	6,569	44,376	47,602
5	20	4,939	44,248	52,086
6	20	5,773	42,879	48,261
1	260	6,578	40,366	47,733
2	260	5,568	46,201	50,272
3	260	7,009	53,217	69,349
4	260	6,175	57,088	67,814
5	260	5,188	41,231	63,253
6	260	6,616	42,818	55,988
1	290	6,227	43,522	56,607
2	290	4,890	43,501	62,743
3	290	6,042	48,215	59,128
4	290	5,632	43,301	63,093
5	290	5,307	38,282	56,144
6	290	6,106	47,990	61,618
1	320	5,258	45,442	59,432
2	320	5,509	40,011	50,797
3	320	5,137	40,503	49,863
4	320	5,704	47,719	54,580
5	320	6,063	45,255	54,490
6	320	4,721	41,693	59,186
1	350	4,949	33,899	47,363
2	350	4,340	38,783	46,409
3	350	5,909	39,543	47,841
4	350	7,470	48,722	62,929
5	350	5,351	43,755	47,505

Preprints (www.preprints.org) | NOT PEER-REVIEWED | Posted: 19 October 2023 doi:10.20944/preprints202310.1275.v1

6	350	6,051	45,896	62,821
1	380	5,147	44,567	58,023
2	380	5,685	45,664	58,818
3	380	5,858	41,558	50,893
4	380	5,859	44,367	53,910
5	380	5,977	46,287	57,900
6	380	6,354	42,925	59,778
1	410	4,659	33,058	36,935
2	410	5,223	38,778	49,032
3	410	6,045	44,076	51,182
4	410	4,886	39,830	64,734
5	410	6,471	43,348	55,387
6	410	5,874	44,498	51,197
1	440	5,773	42,879	48,261
2	440	5,245	38,904	56,476
3	440	5,261	44,417	56,988
4	440	5,688	38,412	47,601
5	440	7,698	50,192	59,783
6	440	5,668	39,901	57,787

Table 3 presents the basic statistical analysis of the surface roughness parameters presented in Table 2.

Table 3. Basic statistical analysis of the results of surface roughness measurements of 48 samples manufactured by selective laser melting technology from AlSi10Mg.

Statistical parameter	Annealing temperature, °C	Ra, µm	Rz, µm	Rmax, µm
Mean value, µm	20	5.804	44.852	57.763
Median, µm		5.885	44.312	50.174
Standard deviation, µm		1.121	7.329	19.173
Maximum value, µm		7.34	54.939	93.837
Minimum value, µm		4.208	33.04	41.141
Mean value, µm	260	6.189	46.820	59.068
Median, µm		6.377	44.510	59.621
Standard deviation, µm		0.692	6.865	9.111
Maximum value, µm		7.009	57.088	69.349
Minimum value, µm		5.188	40.366	47.733
Mean value, µm	290	5.701	44.135	59.889
Median, µm		5.837	43.511	60.373
Standard deviation, µm		0.524	3.667	3.059
Maximum value, µm		6.227	48.215	63.093
Minimum value, µm		4.89	38.282	56.144
Mean value, µm	320	5.399	43.437	54.725
Median, µm		5.384	43.474	54.535
Standard deviation, µm		0.468	3.132	4.030
Maximum value, µm		6.063	47.719	59.432
Minimum value, µm		4.721	40.011	49.863
Mean value, µm	350	5.678	41.766	52.478
Median, µm		5.63	41.649	47.673
Standard deviation, µm		1.080	5.388	8.068
Maximum value, µm		7.47	48.722	62.929
Minimum value, µm		4.34	33.899	46.409

Preprints (www.preprints.org) | NOT PEER-REVIEWED | Posted: 19 October 2023 doi:10.20944/preprints202310.1275.v1

Mean value, μm		5.813	44.228	56.554
Median, μm		5.859	44.467	57.962
Standard deviation, μm	380	0.396	1.747	3.421
Maximum value, μm		6.354	46.287	59.778
Minimum value, μm		5.147	41.558	50.893
Mean value, μm		5.526	40.598	51.411
Median, μm		5.549	41.589	51.190
Standard deviation, μm	410	0.712	4.373	9.040
Maximum value, μm		6.471	44.498	64.734
Minimum value, μm		4.659	33.058	36.935
Mean value, μm		5.889	42.451	54.483
Median, μm		5.678	41.39	56.732
Standard deviation, μm	440	0.915	4.458	5.202
Maximum value, μm		7.698	50.192	59.783
Minimum value, μm		5.245	38.412	47.601

The analysis of basic statistical characteristics shows that the arithmetic mean of absolute values of profile deviations within the basic length (Ra) does not have a wide scatter for different samples. At the same time, the greatest profile height, the sum of the height of the greatest profile protrusion and the depth of the greatest profile depression within the basic length of the sample (Rz) has rather high fluctuations of values from sample to sample, the same behavior is observed for the total profile height (Rmax).

3.2. Mechanical test results for groups of specimens manufactured by selective laser melting technology from AlSi10Mg material, pre-treated at different temperatures.

48 specimens were subjected to tensile tests. 42 of them were pre-annealed at different temperatures. Figure 4 shows the tensile diagrams of samples that did not undergo pre-annealing and samples that underwent pre-annealing at temperatures from 260 to 440 °C.

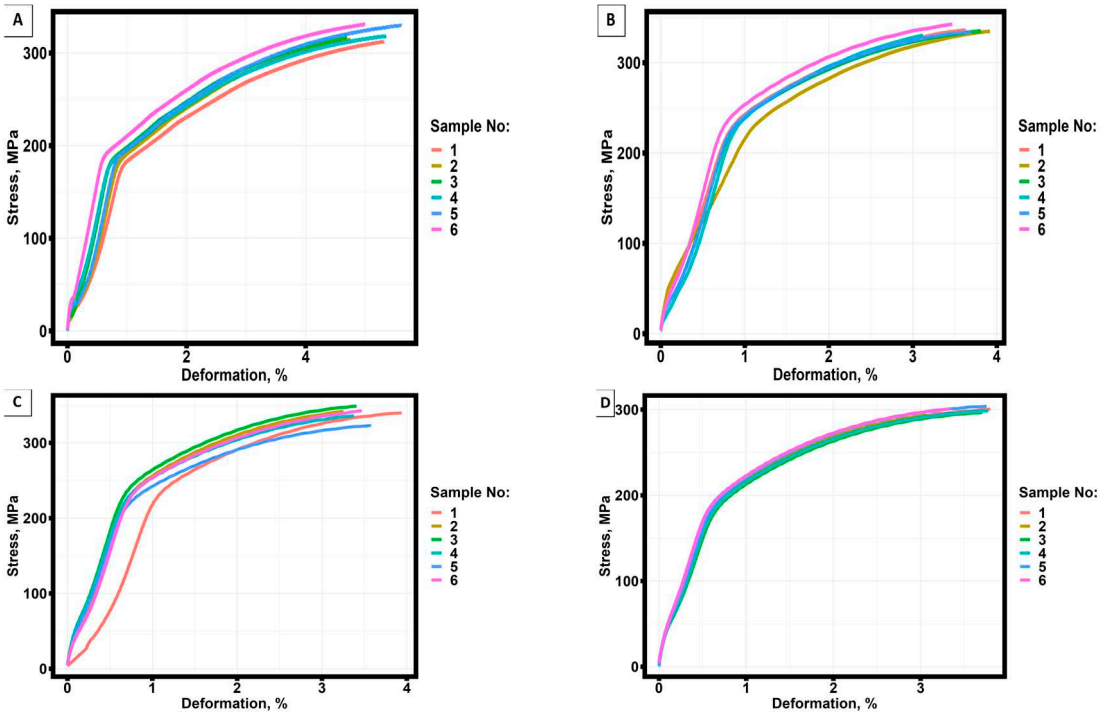

Preprints (www.preprints.org) | NOT PEER-REVIEWED | Posted: 19 October 2023 doi:10.20944/preprints202310.1275.v1

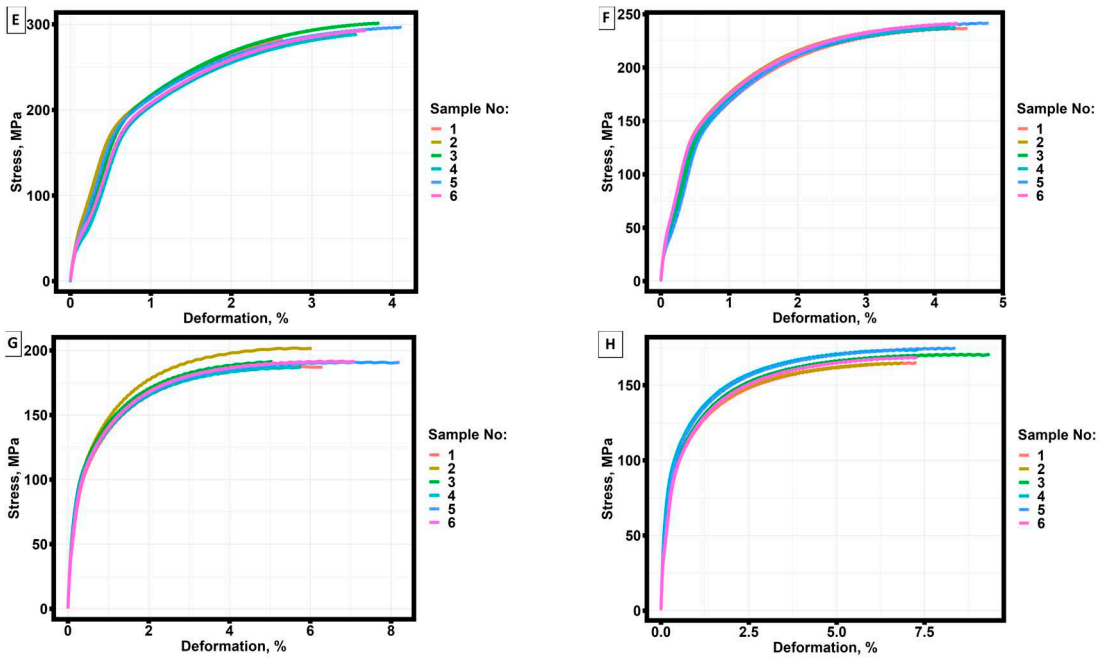

Figure 4. Tensile diagrams of thin-walled samples obtained by selective laser melting technology from AlSi10Mg material with different annealing temperatures. a) without annealing; b) annealing at 260 °C; c) annealing at 290 °C; d) annealing at 320 °C; e) annealing at 350 °C; f) annealing at 380 °C; g) annealing at 410 °C; h) annealing at 440 °C.

Table 4 presents the main mechanical properties of 48 tested samples.

Table 4. Basic mechanical properties of samples obtained by selective laser melting from AlSi10Mg material.

No samples	Annealing temperature, °C	σ0.2, MPa	σU, MPa	ε0.2,%	εU,%
1	20	191.948	308.964	1.173	4.998
2	20	198.216	310.750	1.129	4.478
3	20	194.706	313.314	0.936	4.406
4	20	192.044	314.810	0.928	4.988
5	20	198.825	326.616	1.057	5.222
6	20	200.728	327.219	0.824	4.653
1	260	245.334	328.600	1.036	3.136
2	260	245.452	334.828	1.308	3.919
3	260	247.062	328.213	1.095	3.261
4	260	252.070	321.049	1.169	2.735
5	260	248.233	327.996	1.095	3.170
6	260	253.389	334.916	0.996	2.981
1	290	257.103	333.964	1.383	3.406
2	290	254.805	334.178	0.986	2.791
3	290	257.494	341.998	0.912	2.903
4	290	247.495	328.838	0.922	2.879
5	290	237.288	316.883	0.931	3.025
6	290	253.389	322.998	0.996	2.862
1	320	207.151	294.796	0.869	3.175
2	320	208.406	293.716	0.868	3.074
3	320	204.945	296.520	0.888	3.706
4	320	206.205	298.721	0.862	3.776
5	320	209.819	298.073	0.845	3.136

Preprints (www.preprints.org) | NOT PEER-REVIEWED | Posted: 19 October 2023 doi:10.20944/preprints202310.1275.v1

6	320	208.615	301.139	0.805	3.343
1	350	197.684	283.684	0.749	2.640
2	350	188.093	288.349	0.631	3.194
3	350	204.146	301.434	0.831	3.839
4	350	203.145	288.471	0.975	3.559
5	350	193.197	294.468	0.715	3.710
6	350	198.387	293.003	0.875	3.666
1	380	154.363	235.000	0.789	3.926
2	380	151.798	238.317	0.632	3.744
3	380	153.899	236.487	0.743	3.759
4	380	149.531	235.273	0.647	3.821
5	380	157.501	239.803	0.829	4.186
6	380	149.708	239.161	0.618	3.865
1	410	113.933	186.648	0.543	5.369
2	410	122.491	201.566	0.563	5.230
3	410	115.744	190.155	0.479	4.499
4	410	113.202	186.602	0.504	5.130
5	410	113.399	190.513	0.486	6.981
6	410	115.118	191.084	0.534	6.101
1	440	104.216	164.398	0.600	6.432
2	440	104.979	164.362	0.567	6.293
3	440	107.472	169.422	0.632	7.125
4	440	109.452	173.549	0.516	6.747
5	440	109.941	173.112	0.562	6.346
6	440	106.627	167.986	0.635	6.415

Table 5 presents the basic statistical analysis of mechanical parameters presented in Table 4.

Table 5. Basic statistical analysis of tensile test results of 48 specimens fabricated by selective laser melting technology from AlSi10Mg.

Statistical parameter	Annealing temperature, °C	σ0.2, MPa	σU, MPa	ε0.2,%	εU,%
Mean value	20	196.078	316.946	1.008	4.791
Median		196.461	314.062	0.996	4.821
Standard deviation		3.713	7.986	0.134	0.326
Maximum value		200.728	327.219	1.173	5.222
Minimum value		191.948	308.964	0.824	4.406
Mean value	260	248.590	329.267	1.117	3.200
Median		247.648	328.407	1.095	3.153
Standard deviation		3.407	5.168	0.111	0.397
Maximum value		253.389	334.916	1.308	3.919
Minimum value		245.333	321.049	0.996	2.735
Mean value	290	251.262	329.810	1.021	2.978
Median		254.097	331.401	0.958	2.891
Standard deviation		7.739	8.937	0.181	0.223
Maximum value		257.494	341.998	1.383	3.406
Minimum value		237.288	316.883	0.911	2.791
Mean value	320	207.524	297.161	0.856	3.368
Median		207.779	297.297	0.865	3.259
Standard deviation		1.776	2.719	0.029	0.303
Maximum value		209.819	301.139	0.888	3.776
Minimum value		204.945	293.716	0.805	3.074

Preprints (www.preprints.org) | NOT PEER-REVIEWED | Posted: 19 October 2023 doi:10.20944/preprints202310.1275.v1

Mean value		197.442	291.568	0.796	3.434
Median		198.035	290.737	0.790	3.612
Standard deviation	350	6.064	6.163	0.123	0.447
Maximum value		204.146	301.434	0.975	3.839
Minimum value		188.093	283.684	0.631	2.640
Mean value		152.800	237.340	0.710	3.884
Median		152.849	237.402	0.695	3.843
Standard deviation	380	3.066	2.040	0.090	0.163
Maximum value		157.501	239.803	0.829	4.186
Minimum value		149.531	235	0.618	3.744
Mean value		115.648	191.095	0.518	5.552
Median		114.525	190.334	0.519	5.300
Standard deviation	410	3.496	5.492	0.034	0.868
Maximum value		122.491	201.566	0.563	6.981
Minimum value		113.202	186.602	0.479	4.499
Mean value		107.115	168.805	0.585	6.560
Median		107.050	168.704	0.584	6.424
Standard deviation	440	2.314	4.032	0.046	0.319
Maximum value		109.941	173.549	0.635	7.125
Minimum value		104.216	164.362	0.516	6.293

Preliminary analysis of the results of the basic statistical analysis shows that the maximum value of tensile strength and yield strength is achieved at annealing temperatures of 260 °C and 290 °C, while the maximum ductility is achieved at annealing temperature of 440 °C.

3.3. Statistical analysis of the results.

The choice of the criterion for checking the experimental results for belonging to the normal distribution is made based on calculations of the average statistical power depending on the number of tested samples. The average power of the criteria is calculated using the Monte Carlo method with the number of iterations equal to 100000. During the calculations, a simple distribution was introduced into the criterion, the parameters of which were calculated by the maximum likelihood method. The Cauchy, exponential, Gumbel, log-normal, logistic, normal and Weibull distributions were considered as simple distributions. The distribution parameters were iteratively recalculated depending on the number of tested samples.

Four criteria were selected for the study:

- From parametric criteria:
    - Shapiro-Wilk criteria [51];
    - D'Agostino criteria [52];
- From nonparametric:
    - Kolmogorov-Smirnov criteria [53];
    - Anderson-Darling criteria [54];

Anderson-Darling criterion and D'Agostino criterion have limitations on the minimum number of studies, the number of studies must be greater than or equal to 7.

Figure 5 shows the results of calculating the average power of the statistical criterion depending on the number of trials.

Preprints (www.preprints.org) | NOT PEER-REVIEWED | Posted: 19 October 2023 doi:10.20944/preprints202310.1275.v1

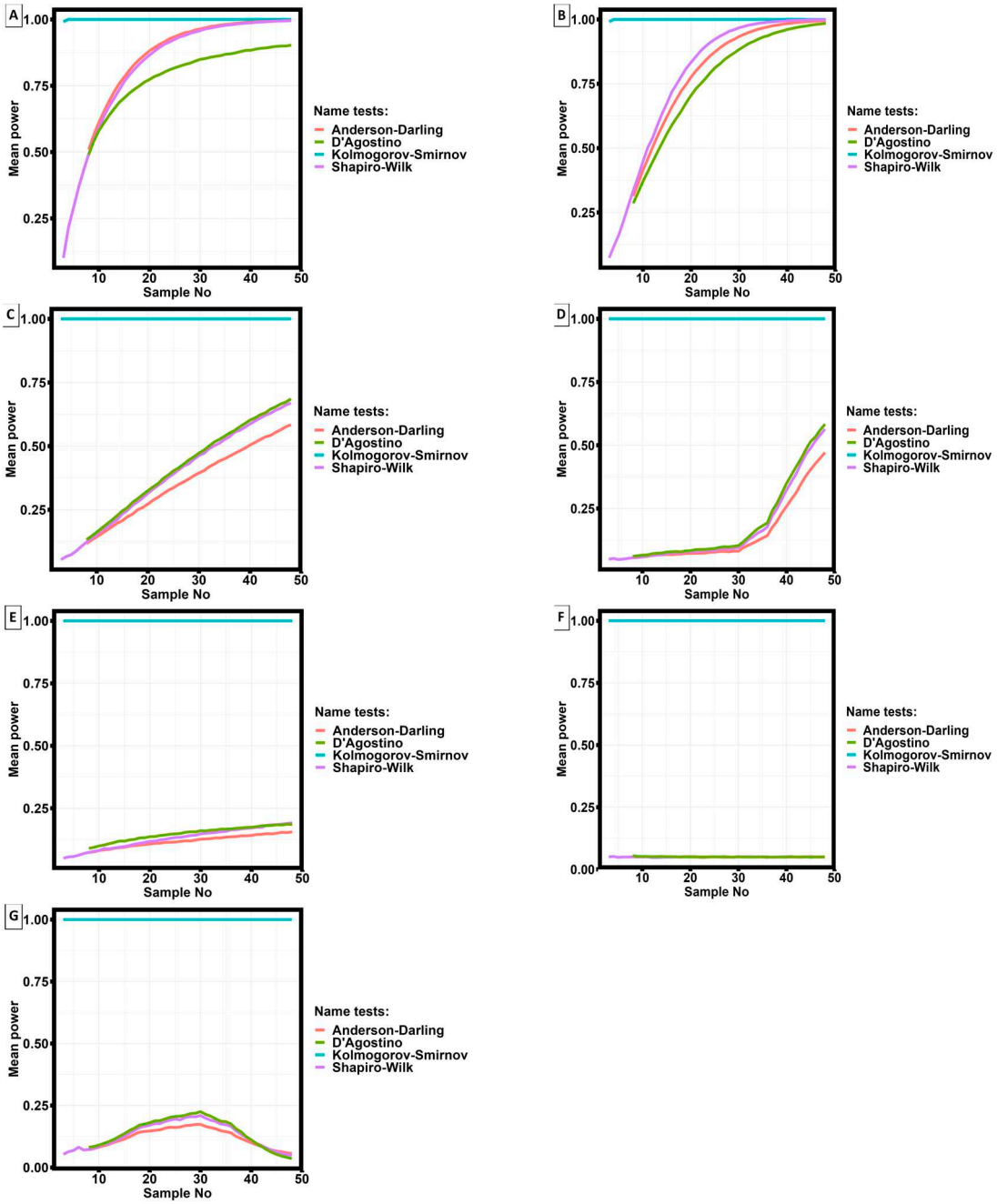

Figure 5. Dependence of the average power of a statistical criterion as a function of the number of trials for four statistical criteria and seven different distributions. (**A**) Cauchy distribution; (**B**) exponential distribution; (**C**) Gumbel distribution; (**D**) log-normal distribution; (**E**) logistic distribution; (**F**) Normal distribution; (**G**) Weibull distribution.

Analysis of the results of calculations of the average statistical power of the four statistical criteria shows that the maximum power is possessed by the Kolmogorov-Smirnov criterion. The exception is the case when the measurement results obey the Cauchy distribution and the exponential distribution, when the number of trials is more than 40, the statistical power of the Anderson-Darling and Shapiro-Wilk criteria is almost equal to the power of the Kolmogorov-Smirnov criterion, and when the number of trials is more than 50, the power of the D'Agostino criterion approaches 1. For other distribution types, the statistical power of the Kolmogorov-Smirnov criterion is maximal.

To determine the theoretical distribution closest to the data, two information criteria were applied: Akaike and Bayesian. The results of applying the Akaike and Bayesian criteria are presented in Table 6.

Preprints (www.preprints.org) | NOT PEER-REVIEWED | Posted: 19 October 2023 doi:10.20944/preprints202310.1275.v1

Table 6. Closest distribution types according to the minimum of Akaike and Bayesian criteria.

Physical parameter	Closest type of distribution
σ0.2 [MPa]	Weibull
σU [MPa]	Weibull
ε0.2,%	Weibull
εU,%	Weibull
Ra, μm	Log-normal
Rz, μm	Logistical
Rmax, μm	Logistical

Thus, the dependence of the average statistical power of the criterion on the number of studies is reflected in Figure 5g and the lowest probability of making an error of the second kind when analyzing the experimental results presented in this paper occurs when using the Kolmogorov-Smirnov criterion.

Considering the results of modeling given in [55,56], the Kolmogorov-Smirnov criterion is the most applicable for data analysis in the problems of materials science, as it has the highest power and does not depend on the type of data distribution (in those cases when the closest type of data distribution are Weibull and Logistic distributions [56]).

Using the Kolmogorov-Smirnov criterion, the data in Tables 2 and 4 were tested for belonging to a normal distribution. Table 7 presents the results of the analysis.

Table 7. Results of testing whether the data in Table 2 and Table 4 belong to a normal distribution.

Kolmogorov - Smirnov statistics	σ0.2, MPa	σU, MPa	ε0.2,%	εU,%	Ra, μm	Rz, μm	Rmax, μm
D	1	1	0.68409	0.99585	0.99999	1	1
p-value	$< 2.2\times 10^{-16}$	$8{,}9\times 10^{-16}$	$< 2.2\times 10^{-16}$	$8{,}9\times 10^{-16}$	$< 2.2\times 10^{-16}$	$< 2.2\times 10^{-16}$	$< 2.2\times 10^{-16}$

Analysis of the results of applying the Kolmogorov-Smirnov test to surface roughness measurements and tensile test results show that the experimental values obtained do not belong to the normal distribution and further statistical analysis should be carried out using non-parametric statistical criteria.

Of practical interest are the correlations between surface roughness parameters and mechanical properties, the change in mechanical properties of samples made by selective laser melting technology and annealing temperature, as well as the behavior of surface roughness as a function of sample length. At the first stage of the analysis, point diagrams of dependence of mechanical properties on surface roughness parameters were plotted.

Figure 6 shows an example of yield strength dependence on surface roughness parameters.

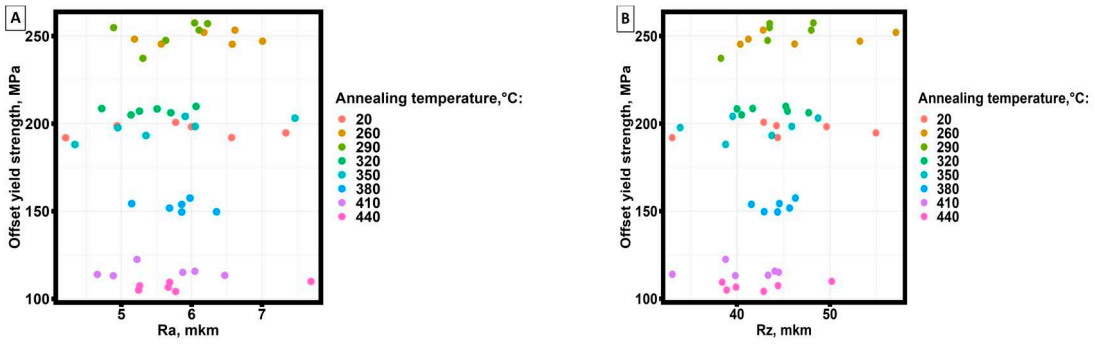

Preprints (www.preprints.org) | NOT PEER-REVIEWED | Posted: 19 October 2023 doi:10.20944/preprints202310.1275.v1

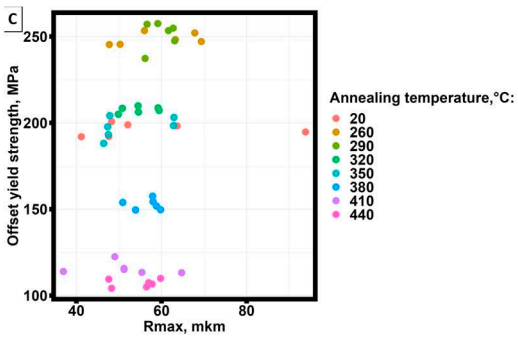

Figure 6. Dependence of yield strength on surface roughness parameters at different annealing temperatures of samples. (a) from Ra; (b) from Rz; (c) from Rmax.

Analysis of the graphs (Figure 6) shows that the yield strength of samples made by selective laser melting technology from AlSi10Mg material practically does not change depending on the main parameters of surface roughness and has a clearly expressed division of data into groups depending on the annealing temperature.

Behavior of the strength limit, strain corresponding to the yield strength and strain corresponding to the strength limit depending on the main parameters characterizing the surface roughness did not show clearly expressed dependencies and stratification into groups.

The differences in the mechanical properties of the samples depending on the annealing temperature were analyzed using the Kruskal-Wallis criterion [57], the results of which are presented in Table 8.

Table 8. Results of applying the Kruskal-Wallis criterion to the data given in Tables 2 and 4 in the study of the influence of annealing temperature on mechanical properties and surface roughness characteristics.

Investigated quantity	Statistical significance level by Kruskal-Wallis test
σ0,2 [MPa]	1.18×10-7
σU [MPa]	1.44×10-7
ε0,2,%	9.89×10-7
εU,%	9.95×10-7
Ra, μm	0.72
Rz, μm	0.67
Rmax, μm	0.43

The results of applying the Kruskal-Wallis criterion show that statistically significant differences are observed in the mechanical properties of samples obtained by selective laser melting technology annealed at different temperatures. No statistically significant differences were found in surface roughness parameters. Comparison of the test results (Table 8) with Figure 6 shows that mechanical properties do not have significant differences at all annealing temperatures.

To test pairwise differences between mechanical properties depending on annealing temperature, the Mann-Whitney test was applied [58]. The results of the test are presented in Table 9.

Table 9. Results of the analysis of statistical differences in groups of samples aged at different temperatures.

Annealing temperature pairs	Results of applying the Mann-Whitney criterion for mechanical properties of samples			
	σ0.2, MPa	σU, MPa	ε0.2,%	εU,%
20 – 260	0.002165	0.008658	0.3095	0.002165
20 – 290	0.002165	0.02597	0.8182	0.002165

Preprints (www.preprints.org) | NOT PEER-REVIEWED | Posted: 19 October 2023 doi:10.20944/preprints202310.1275.v1

20 – 350	0.6991	0.002165	0.04113	0.002165
260 – 290	0.1994	0.9372	0.07765	0.3095
260 – 320	0.002165	0.002165	0.002165	0.3939
260 – 350	0.002165	0.002165	0.002165	0.3939
290 – 350	0.002165	0.002165	0.01515	0.09307
320 – 350	0.002165	0.09307	0.3939	0.5887
350 – 380	0.002165	0.002165	0.2403	0.01515

The results of applying the Mann-Whitney criterion show that statistically significant differences are observed at almost all combinations of annealing temperatures, and all considered mechanical properties, except for aging temperatures 260 ° C and 290 ° C differences in all mechanical properties are not statistically significant. Except for yield strength, the same situation is observed at aging temperatures 320 °C and 350 °C, strength, strain corresponding to yield strength and strain corresponding to tensile strength have no statistically significant differences.

Figure 7 shows the change in the average values of yield strength and tensile strength as a function of annealing temperature, strain corresponding to the tensile strength and yield strength and the change in the strain hardening coefficient ($\theta = \frac{d\sigma}{d\varepsilon}$) [53] in the section of the tensile diagram from yield strength to tensile strength as a function of annealing temperature.

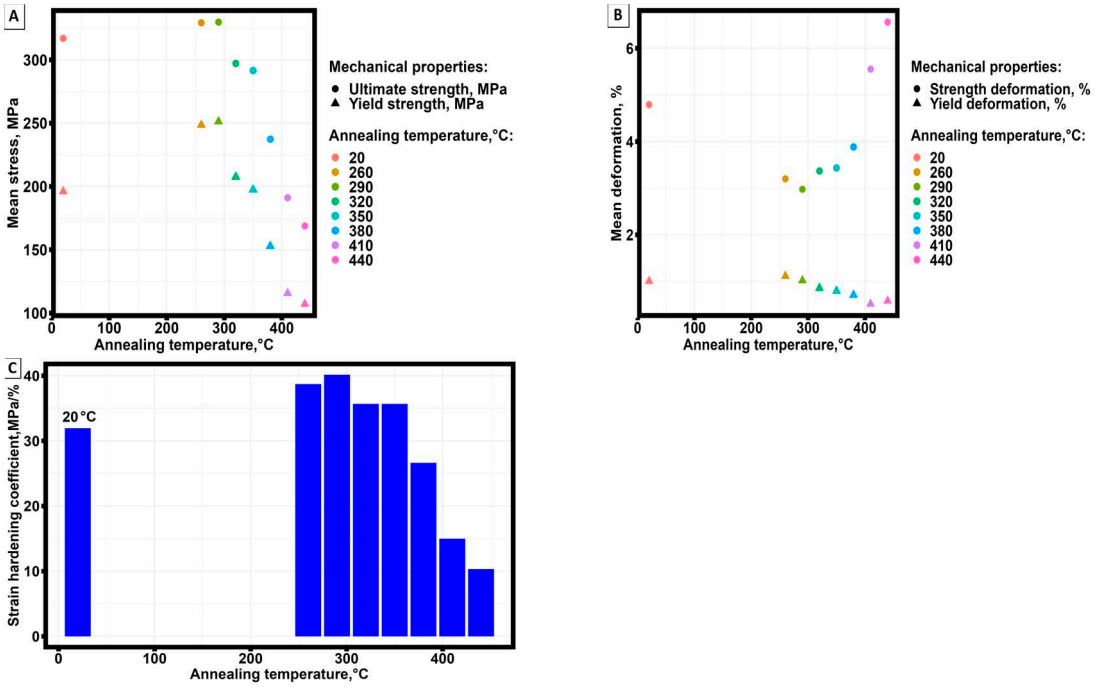

Figure 7. Dependence of average values of strength and yield strengths (**A**), strains corresponding to strength and yield strength (**B**) and strain hardening on aging temperature of samples (**C**) obtained by selective laser melting technology from AlSi10Mg material.

At increase of aging temperature there is a decrease in strength properties and increase in plasticity of samples obtained by selective laser melting technology from AlSi10Mg material (Figure 7a,b).

It follows from the presented dependences (Figure 7c) that the maximum strain hardening is achieved at the aging temperature equal to 290 °C. Considering the results of the analysis given in Table 9, the maximum strain hardening achieved is not statistically significantly different from the strain hardening achieved at 260 °C.

To reveal not clearly expressed dependencies, correlation analysis of mechanical properties of samples obtained by selective laser melting technology from AlSi10Mg material and basic parameters describing surface roughness was applied. Considering the results of analyzing the distributions of

Preprints (www.preprints.org) | NOT PEER-REVIEWED | Posted: 19 October 2023 doi:10.20944/preprints202310.1275.v1

the studied quantities (Table 6 and Table 7, the distribution is different from normal), the correlation analysis by Kendall was applied.

Table 10 shows the Kendall correlation coefficients, the calculated level of statistical significance and the coefficient of determination, the strength of the correlation was interpreted using the Evans scale. The level of statistical significance was assumed to be 0.05.

Table 10. Results of Kendall correlation analysis between the main mechanical properties and surface roughness parameters of the samples obtained by selective laser melting technology from AlSi10Mg material.

Pairs examined for correlation	Kendall correlation coefficient	Statistical significance level	Determination coefficient, %
σ0.2 – Ra	0.2822	0.3282	--
σU – Ra	0.1073171	0.2822	--
ε0,2,% - Ra	0.1259982	0.2069	--
εU, % - Ra	0.09760426	0.3282	--
σ0.2 – Rz	0.1774623	0.07545	--
σU – Rz	0.1676275	0.09298	--
ε0,2,% - Rz	0.2342502	0.01894	5.5
εU, % - Rz	-0.06829269	0.4937	--
σ0.2 – Rmax	0.1792369	0.07257	--
σU – Rmax	0.1268293	0.2037	--
ε0.2,% - Rmax	0.2040816	0.04091	4.2
εU, % - Rmax	-0.1764967	0.07693	--

The results of correlation analysis of mechanical properties of samples manufactured by selective laser melting technology from AlSi10Mg material and basic parameters of surface roughness show the presence of weak statistically significant correlation between the strain corresponding to the yield strength and the sum of the height of the largest profile protrusion and the depth of the largest profile depression within the basic length of the sample (Rz) and between the strain corresponding to the yield strength and the full height of the profile (Rmax), in other cases statistically significant correlation between the strain corresponding to the yield strength and the full height of the profile (Rmax).

Figure 8 shows scatter diagrams of the dependences of the strain corresponding to the yield strength as a function of Rz and Rmax and regression models describing the established dependences.

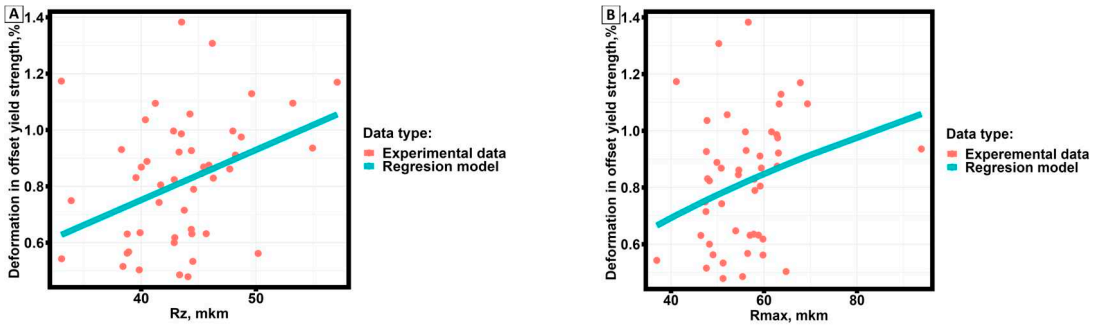

Figure 8. Dependence of strain corresponding to yield strength on (**A**) Rz, (**B**) Rmax and regression models describing the dependence of correlated values.

Table 11 presents the results of constructing the dependence of the strain corresponding to the yield strength on the surface roughness parameters.

Preprints (www.preprints.org) | NOT PEER-REVIEWED | Posted: 19 October 2023 doi:10.20944/preprints202310.1275.v1

Table 11. Equations describing a weak correlation between the strain corresponding to yield strength and surface roughness parameters.

Correlation values		Equations	Standard deviation
ε0,2	Rz	$\varepsilon_{0,2} = 0.0406 + 0.0178 \cdot Rz$	0.1812
	Rmax	$\varepsilon_{0,2} = 0.0033 + 0.1090 \cdot \sqrt[2]{Rmax}$	0.2347

The obtained correlations and regression equations describe a statistically significant relationship between the experimentally obtained data, but do not provide an answer to the causes of the found relationship.

To establish the reasons for the correlation relationship, the sum of the heights of the largest protrusions and depths of the largest depressions of the surface roughness profile within the base length of the sample (Rz) and the total height of the surface roughness profile (Rmax) were analyzed.

Rz is calculated by the equation:

$$Rz = \frac{\sum_{i=1}^{5}|y_{pmi}| + \sum_{i=1}^{5}|y_{vmi}|}{5} \quad (1)$$

where y_{pmi} – height of the i-th protrusion of the surface roughness profile; y_{vmi} – depth of the i-th depression of the surface roughness profile.

Rmax, respectively:

$$Rmax = |y_{max} - y_{min}| \quad (2)$$

where y_{max} – maximum height of roughness profile; y_{min} – maximum depth of surface roughness profile.

The analysis of the values included in equations (1) and (2) shows that the main variables have extreme character and their behavior should be analyzed by means of extreme value analysis [60]. However, it should be taken into account that the correlation is observed with the value characterizing the sample as a whole and the analysis should be performed based on the influence of extreme values on each other.

For these purposes, the autocorrelation function of the extreme values of the surface roughness profile was analyzed. As a result of the analysis it was found that statistically significant autocorrelation of maxima and minima is observed only for two samples - sample No. 3, aged at 380 °C and sample No. 4 aged at 440 °C. Figure 9 shows the graphs of autocorrelation functions of maxima and minima for these samples.

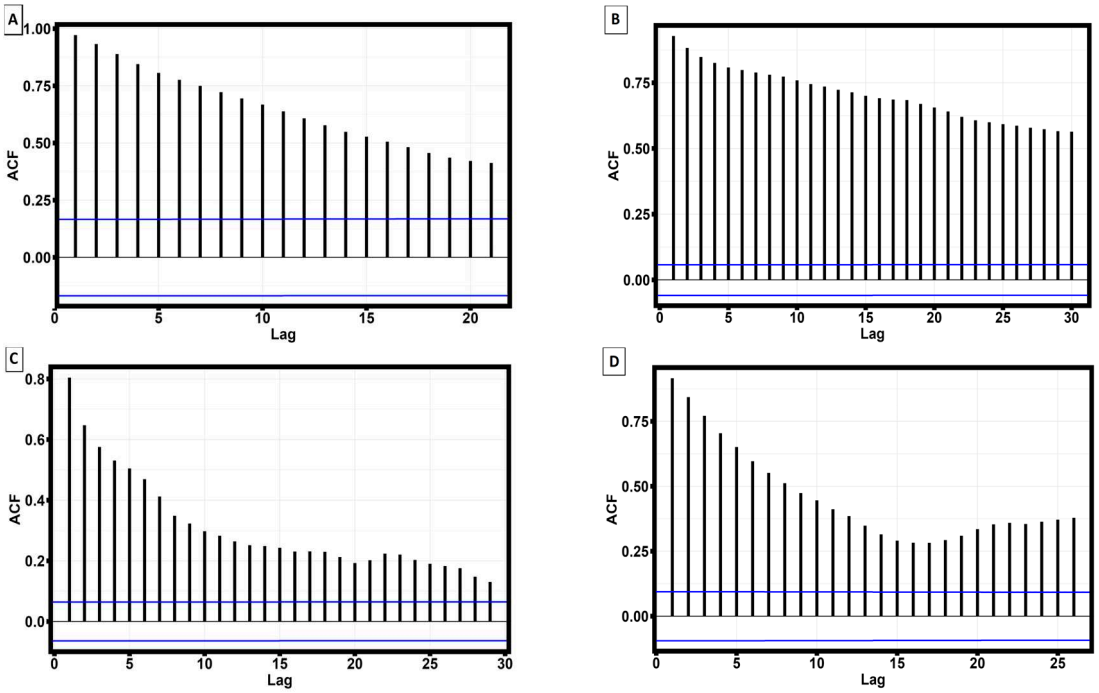

 doi:10.20944/preprints202310.1275.v1

Figure 9. Autocorrelation functions of minima and maxima of the surface roughness profile. a) ACF minima of sample No 4 aging at 440 °C; b) ACF maxima of sample No 4 aging at 440 °C; c) ACF minima of sample No 3 aging at 380 °C; d) ACF minima of sample No 3 aging at 380 °C.

Removal of sample No. 3 aged at 380 °C and sample No. 4 aged at 440 °C from the total sample leads to the fact that the correlation between the strain corresponding to the yield strength and roughness parameters Rz and Rmax becomes statistically insignificant. Thus, the positive influence of surface roughness on the strain corresponding to the yield strength occurs when the maxima and minima of the surface roughness profile have a significant statistical correlation along the entire length of the sample.

4. Conclusions

As a result of statistical analysis of changes in mechanical properties and surface roughness depending on heat treatment, it was found that:

1. Maximum strain hardening of thin-walled samples made by selective laser melting technology from AlSi10Mg is achieved during heat treatment for 1 hour at 290 °C.
2. The mechanical properties of AlSi10Mg samples are not statistically significantly different at 260 °C and 290 °C.
3. At heat treatment of samples in the temperature range from 290 °C to 440 °C within one hour there are no statistically significant changes in surface roughness.
4. The correlation between the deformation corresponding to the yield strength and the sum of heights of the largest protrusions and depths of the largest depressions of the surface roughness profile within the basic length of the sample (Rz) and the full height of the surface roughness profile (Rmax) has been established.
5. The reason for the correlation is the stationary behavior of the maxima and minima of the surface roughness profile along the entire length of the specimens.

Summarizing the results of the studies, we can conclude that low-temperature heat treatment regimes, carried out within 1 hour, allow to achieve strain hardening of thin-walled AlSi10Mg samples. Considering the previously conducted studies it is necessary to continue the search for heat treatment modes and parameters of manufacturing samples by SLM method to obtain surface roughness, positively affecting the mechanical properties.

Author Contributions: Conceptualization, N.N., P.P.; methodology, N.N., P.P., O.K.; software, N.N., O.Y., O.K.; validation, N.N., O.K.; formal analysis, P.P., N.N., I.I.; investigation, R.K., I.I.; resources, N.N., O.Y.; data curation, N.K., O.Y., O.K; writing—original draft preparation, N.N., P.P..; writing—review and editing, N.N., P.P.; visualization, P.P., N.K., O.Y..; supervision, S.N.G., N.K.; project administration, S.N.G., P.P.; funding acquisition, P.P., N.K., O.Y. All authors have read and agreed to the published version of the manuscript.

Funding: This work was supported by the Ministry of Health of the Russian Federation under project 056-00041-23-00.

Data Availability Statement: Not applicable.

Acknowledgments: This work was carried on the equipment of the Collective Use Center of MSTU "STANKIN" (project No. 075-15-2021-695).

Conflicts of Interest: The authors declare no conflict of interest.

References

1. International Organization for Standardization. ISO/ASTM 52900:2015 [ASTM F2792] Additive Manufacturing-General Principles-Terminology; ISO: Geneva, Switzerland, 2015.
2. Ian Gibson, David Rosen, Brent Stucker. Additive Manufacturing Tecnologies. 3D Printing, Rapid Prototyping and Direct Digital Manufacturing//Springer, 2015 – P.P. 648
3. Sandeep Rauta, Vijaykumar S. Jattib, Nitin K. Khedkarc, T.P.Singhd. Investigation of the effect of built orientation on mechanical properties and total cost of FDM parts // Procedia materials science 6 (2014) 1625-1630

4. Ludmila Novakova - Marcincinova, Jozef Novak - Marcincin. Verification of mechanical Properties of ABS materials used in FDM rapid prototyping technology// Proceedings in manufacturing systems/vol. 8. ISS. 2. 2013. 87-92.
5. P. Dudek. FDM 3D printing technology in manufacturing composite elements. Archives of metallurgy and materials// vol. 58. 2013/ ISS.4/dol.: 10.2478/AMM-2013-0186
6. Borgue, R. 3D printing: the dawn of a new era in manufacturing? / R. Borgue // Assembly Automation. 2013. Vol. 33. ¹4. P. 307-311.
7. S.A.M. Tofail, E.P. Koumoulos, A. Bandyopadhyay, S. Bose, L. O'Donoghue, C. Charitidis, Additive manufacturing: scientific and technological challenges, market uptake and opportunities, Mater. Today 21 (2018) 22e37.
8. J.M. Lee, S.L. Sing, M.M. Zhou, W.Y. Yeong, 3D bioprinting processes: a perspective on classification and terminology, Int. J. Bioprint. 4 (2) (2018) 151.
9. J. Haubrich, J. Gussone, P. Barriobero-Vila, P. Kürnsteiner, E.A. Jagle, D. Raabe, € N. Schell, G. Requena, The role of lattice defects, element partitioning and intrinsic heat effects on the microstructure in selective laser melted Ti-6Al-4V, Acta Mater. 167 (2019) 136e148.
10. T. DebRoy, H.L. Wei, J.S. Zuback, T. Mukherjee, J.W. Elmer, J.O. Milewski, A.M. Beese, A. Wilson-Heid, A. De, W. Zhang, Additive manufacturing of metallic componentseprocess, structure and properties, Prog. Mater. Sci. 92 (2018) 112e224.
11. Khmyrov, R.S.; Grigoriev, S.N.; Okunkova, A.A.; Gusarov, A.V. On the possibility of selective laser melting of quartz glass. Phys. Procedia. 2014, 56, 345.
12. Khmyrov, R.S.; Protasov, C.E.; Grigoriev, S.N.; Gusarov, A.V. Crack-free selective laser melting of silica glass: single beads and monolayers on the substrate of the same material. Int. J. Adv. Manuf. Technol. 2016, 85, 1461-69. (Publons 43)
13. Protasov, C.E.; Khmyrov, R.S.; Grigoriev, S.N.; Gusarov, A.V. Selective laser melting of fused silica: Interdependent heat transfer and powder consolidation. Int. J. Heat Mass Transf. 2017, 104, 665-674.
14. Grigoriev, S.N.; Volosova, M.A.; Peretyagin, P.Y.; Seleznev, A.E.; Okunkova, A.A.; Smirnov, A. The Effect of TiC Additive on Mechanical and Electrical Properties of Al2O3 Ceramic. Appl. Sci. 2018, 8, 2385.
15. Gusarov, A.V.; Grigoriev, S.N.; Volosova, M.A.; Melnik, Y.A.; Laskin, A.; Kotoban, D.V.; Okunkova, A.A. On productivity of laser additive manufacturing. J. Mater. Process. Technol. 2018, 261, 213.
16. H. Asgari, A. Odeshi, K. Hosseinkhani, M. Mohammadi, On dynamic mechanical behavior of additively manufactured AlSi10Mg_200C, Mater. Lett. 211 (2018) 187e190.
17. Y. Chen, J.X. Zhang, X.H. Gu, N.W. Dai, P. Qin, L.C. Zhang, Distinction of corrosion resistance of selective laser melted Al-12Si alloy on different planes, J. Alloys Compd. 747 (2018) 648-658.
18. Leon, Avi, and Eli Aghion. "Effect of surface roughness on corrosion fatigue performance of AlSi10Mg alloy produced by Selective Laser Melting (SLM)." Materials Characterization 131 (2017): 188-194. https://doi.org/10.1016/j.matchar.2017.06.029
19. Rosenthal, Idan, Adin Stern, and Nachum Frage. "Microstructure and mechanical properties of AlSi10Mg parts produced by the laser beam additive manufacturing (AM) technology." Metallography, Microstructure, and Analysis 3 (2014): 448-453. https://doi.org/10.1007/s13632-014-0168-y
20. Kamarudin, K., et al. "Dimensional accuracy and surface roughness analysis for AlSi10Mg produced by selective laser melting (SLM)." MATEC Web of Conferences. Vol. 78. EDP Sciences, 2016. https://doi.org/10.1051/matecconf/20167801077
21. Zhichao Dong, Yabo Liu, Weijie Li, Jun Liang, Orientation dependency for microstructure, geometric accuracy and mechanical properties of selective laser melting AlSi10Mg lattices //Journal of Alloys and Compounds, 791 (2019): 490-500, ISSN 0925-8388, https://doi.org/10.1016/j.jallcom.2019.03.344.
22. Mertens, Anne, et al. "Microstructure and properties of SLM AlSi10Mg: understanding the influence of the local thermal history." Procedia Manufacturing 47 (2020): 1089-1095. https://doi.org/10.1016/j.promfg.2020.04.121
23. Kempen, Karolien, et al. "Mechanical properties of AlSi10Mg produced by selective laser melting." Physics Procedia 39 (2012): 439-446. https://doi.org/10.1016/j.phpro.2012.10.059
24. Jing, C. H. E. N., et al. "Microstructure, porosity and mechanical properties of selective laser melted AlSi10Mg." Chinese Journal of Aeronautics 33.7 (2020): 2043-2054. https://doi.org/10.1016/j.cja.2019.08.017
25. Rakesh, Ch Srinivasa, et al. "Effect of build atmosphere on the mechanical properties of AlSi10Mg produced by selective laser melting." Materials Today: Proceedings 5.9 (2018): 17231-17238. https://doi.org/10.1016/j.matpr.2018.04.133
26. Praneeth, Jammula, Sriram Venkatesh, and L. Sivarama Krishna. "Process parameters influence on mechanical properties of AlSi10Mg by SLM." Materials Today: Proceedings (2023). https://doi.org/10.1016/j.matpr.2022.12.222
27. Aboulkhair, Nesma T., et al. "Reducing porosity in AlSi10Mg parts processed by selective laser melting." Additive manufacturing 1 (2014): 77-86. https://doi.org/10.1016/j.addma.2014.08.001

28. Limbasiya, Nandita, et al. "A comprehensive review on the effect of process parameters and post-process treatments on microstructure and mechanical properties of selective laser melting of AlSi10Mg." Journal of Materials Research and Technology (2022). https://doi.org/10.1016/j.jmrt.2022.09.092
29. Maleki, Erfan, Sara Bagherifard, and Mario Guagliano. "Correlation of residual stress, hardness and surface roughness with crack initiation and fatigue strength of surface treated additive manufactured AlSi10Mg: Experimental and machine learning approaches." Journal of Materials Research and Technology 24 (2023): 3265-3283. https://doi.org/10.1016/j.jmrt.2023.03.193
30. Majeed, Arfan, et al. "Surface quality improvement by parameters analysis, optimization and heat treatment of AlSi10Mg parts manufactured by SLM additive manufacturing." International Journal of Lightweight Materials and Manufacture 2.4 (2019): 288-295. https://doi.org/10.1016/j.ijlmm.2019.08.001
31. Wei, Pei, et al. "The AlSi10Mg samples produced by selective laser melting: single track, densification, microstructure and mechanical behavior." Applied surface science 408 (2017): 38-50. https://doi.org/10.1016/j.apsusc.2017.02.215
32. Ammar, H. R., A. M. Samuel, and F. H. Samuel. "Porosity and the fatigue behavior of hypoeutectic and hypereutectic aluminum–silicon casting alloys." International journal of Fatigue 30.6 (2008): 1024-1035. https://doi.org/10.1016/j.ijfatigue.2007.08.012
33. Yu, Wenhui, et al. "Influence of re-melting on surface roughness and porosity of AlSi10Mg parts fabricated by selective laser melting." Journal of Alloys and Compounds 792 (2019): 574-581. https://doi.org/10.1016/j.jallcom.2019.04.017
34. Yang, Tao, et al. "Effect of processing parameters on overhanging surface roughness during laser powder bed fusion of AlSi10Mg." Journal of Manufacturing Processes 61 (2021): 440-453. https://doi.org/10.1016/j.jmapro.2020.11.030
35. Boschetto, Alberto, Luana Bottini, and Francesco Veniali. "Roughness modeling of AlSi10Mg parts fabricated by selective laser melting." Journal of Materials Processing Technology 241 (2017): 154-163. https://doi.org/10.1016/j.jmatprotec.2016.11.013
36. Yang, Tao, et al. "The influence of process parameters on vertical surface roughness of the AlSi10Mg parts fabricated by selective laser melting." Journal of Materials Processing Technology 266 (2019): 26-36. https://doi.org/10.1016/j.jmatprotec.2018.10.015
37. Read, Noriko, et al. "Selective laser melting of AlSi10Mg alloy: Process optimisation and mechanical properties development." Materials & Design (1980-2015) 65 (2015): 417-424. https://doi.org/10.1016/j.matdes.2014.09.044
38. Wang, Lin-zhi, Sen Wang, and Jiao-jiao Wu. "Experimental investigation on densification behavior and surface roughness of AlSi10Mg powders produced by selective laser melting." Optics & Laser Technology 96 (2017): 88-96. https://doi.org/10.1016/j.optlastec.2017.05.006
39. Han, Xuesong, et al. "Investigation on selective laser melting AlSi10Mg cellular lattice strut: Molten pool morphology, surface roughness and dimensional accuracy." Materials 11.3 (2018): 392. https://doi.org/10.3390/ma11030392
40. Li, Bao-Qiang, et al. "Research on surface roughness of AlSi10Mg parts fabricated by laser powder bed fusion." Metals 8.7 (2018): 524. https://doi.org/10.3390/met8070524
41. Zyguła, Krystian, et al. "Mechanical properties and microstructure of AlSi10Mg alloy obtained by casting and SLM technique." World Scientific News 104 (2018): 456-466.
42. Maleki, Erfan, Sara Bagherifard, and Mario Guagliano. "Correlation of residual stress, hardness and surface roughness with crack initiation and fatigue strength of surface treated additive manufactured AlSi10Mg: Experimental and machine learning approaches." Journal of Materials Research and Technology 24 (2023): 3265-3283. https://doi.org/10.1016/j.jmrt.2023.03.193
43. Schneller, Wolfgang, et al. "Effect of post treatment on the microstructure, surface roughness and residual stress regarding the fatigue strength of selectively laser melted AlSi10Mg structures." Journal of Manufacturing and Materials Processing 3.4 (2019): 89. https://doi.org/10.3390/jmmp3040089
44. Yadroitsev, I.; Bertrand, Ph.; Antonenkova, G.; Grigoriev, S.; Smurov, I. Use of track/layer morphology to develop functional parts by selectivelaser melting. J. Laser Appl. 2013, 25, 052003. (Publons 55)
45. Trevisan, Francesco, et al. "On the selective laser melting (SLM) of the AlSi10Mg alloy: process, microstructure, and mechanical properties." Materials 10.1 (2017): 76. https://doi.org/10.3390/ma10010076
46. Aboulkhair, Nesma T., et al. "The microstructure and mechanical properties of selectively laser melted AlSi10Mg: The effect of a conventional T6-like heat treatment." Materials Science and Engineering: A 667 (2016): 139-146. https://doi.org/10.1016/j.msea.2016.04.092
47. Patakham, U., et al. "MPB characteristics and Si morphologies on mechanical properties and fracture behavior of SLM AlSi10Mg." Materials Science and Engineering: A 821 (2021): 141602. https://doi.org/10.1016/j.msea.2021.141602
48. E.V. Shelekhov, T.A. Sviridova, Programs for X-rayanalysis of polycrystals, Metal Sci. Heat Treat. 42 (2000)309–313

49. S. Grazulis, D. Chateigner, R.T. Downs, A.T. Yokochi, M.Quiros, L. Lutterotti, E. Manakova, J. Butkus, P. Moeck, A.Le Bail, Crystallography open database an open-accesscollection of crystal structures, J. Appl. Cryst. 42 (2009) 726–729
50. Kashyap, Anil, ed. Dynamic stochastic models from empirical data. Academic Press, 1976.
51. Shapiro, S.S.; Wilk, M.B. An analysis of variance test for normality. Biom. Trust 1965, 52, 591–611.
52. D'Agostino, Ralph B.; Pearson, E. S. (1973). "Tests for Departure from Normality. Empirical Results for the Distributions of b2 and √b1". Biometrika. 60 (3): 613–622.
53. Kolmogorov, A.N. Sulla determinazione empirica di une legge di distribuzione. G. Ist. Ital. Attuari 1933, 4, 83–91.
54. W. Anderson, On the Distribution of the Two-Sample Cramer-von Mises Criterion// Ann. Math. Statist. 33(3): 1148-1159 (September, 1962).
55. Smirnov, A.; Nikitin, N.; Peretyagin, P.; Khmyrov, R.; Kuznetsova, E.; Solis Pinargote, N.W. Experimental and Statistical Modeling for Effect of Nozzle Diameter, Filling Pattern, and Layer Height of FDM-Printed Ceramic–Polymer Green Body on Biaxial Flexural Strength of Sintered Alumina Ceramic. J. Compos. Sci. 2023, 7, 381. https://doi.org/10.3390/jcs7090381
56. Skorodumov, S.V.; Neganov, D.A.; Studenov, E.P.; Poshibaev, P.V.; Nikitin, N.Y. Statistical analysis of mechanical test results for samples of pipes from trunk oil pipelines after long-term operation. Industr. Lab. Diagn. Mater. 2022, 88, 82–91.
57. Kruskal, W.H.; Wallis, W.A. Use of ranks in one-criterion variance analysis. J. Am. Stat. Assoc. 1952, 47, 583–621.
58. Mann, Henry B., and Donald R. Whitney. "On a test of whether one of two random variables is stochastically larger than the other." The annals of mathematical statistics (1947): 50-60.
59. Bannykh I.O., Sevostyanov M.A., Prutskov M.E. Investigation of heat treatment effect on mechanical properties and structure of high-nitrogen austenitic steel 02Kh20AG10N4MFB. Russian Metallurgy (Metally) volume 4(2016), pp. 39-44.
60. Benstock, Daniel, and Frederic Cegla. "Extreme value analysis (EVA) of inspection data and its uncertainties." Ndt & E international 87 (2017): 68-77.